PERIODICO di MINERALOGIA
established in 1930

An International Journal of
Mineralogy, Crystallography, Geochemistry,
Ore Deposits, Petrology, Volcanology
and applied topics on Environment, Archaeometry and Cultural Heritage

The role of calcium-based additives in extracting iron from red mud through carbothermic reduction

Bambang Suharno [1], Celvin Salim [1], Najwan Hikaman Kamil [1], Tiara Nur Salsabila [2], Soesaptri Oediyani [2], Donny Zulfakar [3], Titin Siti Fatimah [4], Nuryadi Saleh [4], Sariman [5], Harta Haryadi [5], Fajar Nurjaman [5,*]

[1] Universitas Indonesia, Department of Metallurgical and Materials, Depok, Indonesia
[2] Department of Metallurgical Engineering, Universitas Sultan Ageng Tirtayasa, Cilegon, Indonesia
[3] Mining Industry Indonesia (MIND ID), Jakarta, Indonesia
[4] Testing Center for Mineral and Coal, Ministry of Energy and Mineral Resources, Indonesia
[5] National Research and Innovation Agency, Research Center for Mineral Technology, South Lampung, Indonesia

ARTICLE INFO

Submitted: October 2025
Accepted: March 2026
Available on line: April 2026

* Corresponding author:
fajar.nurjaman@brin.go.id

Doi: 10.13133/2239-1002/19105

How to cite this article:
Suharno B. et al. (2026)
Period. Mineral. 95, 157-168

ABSTRACT

Increasing aluminum demand has increased the red mud, a bauxite residue of the Bayer process. It contains valuable elements, such as iron, titanium, vanadium, and a small amount of rare-earth elements. Utilization of red mud is required to prevent environmental damage. In this work, the carbothermic reduction was followed by magnetic separation of red mud to extract iron. The effects of calcium-based additives, i.e., $CaCl_2$ and CaF_2, on recovery and metallization degree, as well as on phase transformation and morphology of iron particles in reduced pellets, were investigated. The red mud, coal, and additives were mixed homogeneously and pelletized into a diameter of 10 mm. The reduction process was carried out in a muffle furnace at 1050-1250 °C for 60 minutes. Furthermore, the reduced pellet was ground and a magnetic separation process was conducted to separate the iron metal from its gangue. The results showed that CaF_2 performed better than $CaCl_2$. The optimum result was obtained by adding 8% CaF_2 and a 1.0 stoichiometric amount of coal to the carbothermic reduction of red mud at 1250 °C for 60 minutes. It generated iron grade, recovery, and metallization of 83.64%, 98%, and 93.5%, respectively.

Keywords: red mud; carbothermic reduction; magnetic separation; calcium chloride; calcium fluoride.

INTRODUCTION

Aluminum demand is the second-largest after steel, growing rapidly due to its essential role in construction, transportation, energy, electronics, and food packaging (Yi et al., 2024). It was produced by processing alumina obtained from bauxite via the Bayer process. The process produced 1 ton of solid residue, called red mud, from 2 tons of alumina (Bhoi et al., 2017). It has high alkalinity and contains heavy metals, such as iron, titanium, and vanadium, as well as a small amount of rare-earth elements (cerium, scandium, and lanthanum) (Swain et al., 2020). Its disposal into the land or ocean will harm the environment (Wang and Liu, 2021). Therefore, it is important to utilize red mud to solve this problem (Wang et al., 2021). Extracting iron from red mud containing 30-60 wt% iron-bearing compounds (Fe_2O_3, FeOOH and $FeTiO_3$) could be an alternative resource in ironmaking (Mombelli et al., 2019; Arroyo et al., 2020). Upgrading iron in red mud via a beneficiation route cannot be carried out due to the fine particles and complex structural compounds. Pyrometallurgy is the standard process to extract iron directly from red mud.

Researchers reported that smelting red mud at 1500-1750 °C is required to achieve good separation between metallic iron and slag (Balomenos et al., 2014; Borra et al., 2016; Valeev et al., 2020; Ning et al., 2018). Nevertheless, high impurity levels and low Fe total content in red mud have become economically challenging in this work (Paramguru et al., 2004; Liu et al., 2021). Carbothermic reduction followed by a low-intensity magnetic separation process has been developed (Agrawal et al., 2018). Low-temperature processes and the flexibility in reductant use have made this technology more reliable for producing metallic iron from red mud (Samouhos et al., 2017). Sadangi et al. (2018) reported that carrying out carbothermic reduction on a red mud containing 46.95% of Fe_2O_3 at 1150 °C for 60 minutes, followed by a magnetic separation process using 0.18 T, produced 65.93% and 61.85% for iron grade and recovery, respectively. Nevertheless, the low-quality product generated by this method is due to the high SiO_2 content in red mud, which may cause iron oxide to react with SiO_2 to form iron silicate, which is more difficult to reduce to metallic iron than iron oxide. Therefore, higher temperature reduction, mostly at 1200 °C or above, should be used to achieve high metallic yield and iron recovery (Eray et al., 2021).

Some additives were used to improve the iron grade and recovery at low-temperature reduction. Many researchers have used sodium salts as additives to improve iron extraction from red mud. Zhu et al. (2012) used sodium carbonate to obtain metallic iron from red mud. However, iron will react with silicon at elevated temperatures to form iron silicate, reducing iron's recovery and metallization. Grudinsky et al. (2021) used sodium sulfate, which could inhibit the formation of iron silicate in the carbothermic reduction of red mud. Aluminum and silica minerals in red mud will be reacted with sodium to form gehlenite ($Ca_2Al_2SiO_7$), albite ($NaCaAlSiO_7$) and andradite ($Ca_3Al_2(SiO_4)_3$) during the carbothermic reduction process (Ding et al., 2020). In addition, it also promoted the grain growth of iron particles. The agglomeration of this particle occurred due to the formation of a low-melting-point phase of iron-sulfur compounds, which could enhance mass transport and diffusion rates. Large iron particles improved impurity liberation, resulting in high iron recovery after grinding and continued magnetic separation. Chun et al. (2013) also reported that using sodium sulfate and calcium oxide yielded 92.14% and 94.87% recovery and metallization of iron, respectively, when red mud was heated to 1150 °C for 80 minutes. The lower temperature reduction process of red mud with the presence of a mixture of 6% of sodium sulfate and 6% of sodium carbonate was carried out by Li et al. (2014), where 95% of iron recovery was obtained from carbothermic reduction of red mud at 1050 °C for 60 minutes. However, adding sodium sulfate resulted in metallic iron containing high sulfur content. The use of calcium salts as additives in carbothermic reduction of red mud is still less investigated. The use of calcium oxide in the dealkalization of red mud has been reported by Zhou et al. (2024). Calcium oxide can also react with silicon to form calcium silicate or diopside, which hinders iron silicate formation. Therefore, in this work, two types of calcium salts (chloride and fluoride) were studied to determine their effects on iron extraction via carbothermic reduction, followed by magnetic separation.

METHODS

Materials

Red mud was obtained from the alumina industry in Kalimantan, Indonesia. The XRF analysis was performed to determine the chemical composition of red mud. From Table 1, the red mud contains 25.13% of total iron and high quartz and alumina content, which cannot be smelted directly in a Blast Furnace (Dmitriev, 2018). From XRD analysis (Figure 1), iron is present as hematite (Fe_2O_3) and goethite [(Fe,Al)OOH]. Quartz (SiO_2) was observed as a major impurity in red mud. Silicate compounds are present in the form of natrolite [$Na_2Al_2Si_3O_{10}(OH)_4$] and chantalite [$CaAl_2SiO_4(OH)_4$]. They are generated by alkali digestion and calcination in the Bayer process, respectively. Natrolite will transform into nepheline ($NaAlSiO_4$) during the carbothermic process at high temperature. It has a low melting temperature, which positively affects iron extraction from red mud. Chantalite will transform into calcium carbonate, which can be reacted with SiO_2 to form diopside ($CaSiO_3$) (Yadav et al., 2010).

In this experiment, 6.13 g of coal containing 65.55% of fixed carbon was added following the stoichiometric calculation of carbon required from Reaction (1) to generate CO gas to reduce iron oxide into metallic iron, as expressed from Reactions (2-5). The proximate, ash composition and sulfur content of coal are listed in Table 2. All additives

Table 1. Chemical composition of red mud (wt%).

Fe (total)	Fe_2O_3	SiO_2	Al_2O_3	CaO	TiO_2	MnO	K_2O
25.13	62.94	15.07	14.50	1.46	1.03	0.18	0.39

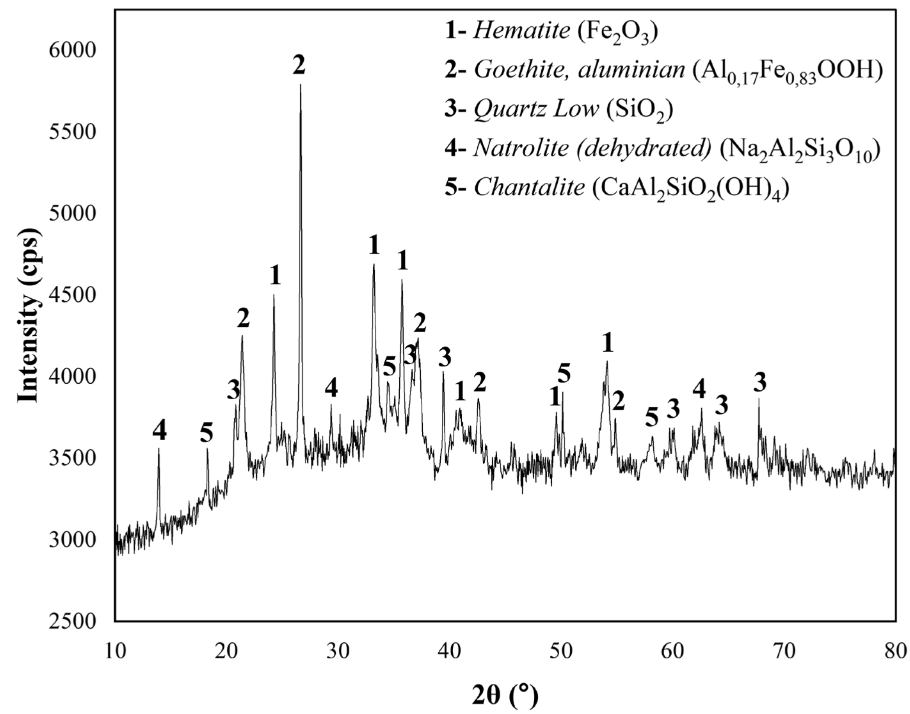

Figure 1. XRD analysis of red mud.

($CaCl_2$ and CaF_2) used in this experiment were analytical grade.

$$C+CO_{2(g)}\rightarrow 2CO_{(g)} \quad (1)$$

$$(Fe,Al)OOH\rightarrow 2(Fe,Al)_2O_3+H_2O_g \quad (2)$$

$$3Fe_2O_3+CO_2\rightarrow 2Fe_3O_4+CO_{2(g)} \quad (3)$$

$$Fe_3O_4+CO_{(g)}\rightarrow 3FeO+CO_{2(g)} \quad (4)$$

$$FeO+CO_{(g)}\rightarrow Fe+CO_{2(g)} \quad (5)$$

$$FeO+Al_2O_3\rightarrow FeAl_2O_4 \quad (6)$$

$$Na_2Al_2Si_3O_{10}\cdot 2H_2O\rightarrow 2NaAlSiO_4+SiO_2+2H_2O_{(g)} \quad (7)$$

$$CaAl_2S_4\cdot 2H_2O\rightarrow CaAl_2SiO_4+2H_2O_{(g)} \quad (8)$$

Experimental

Fine red mud was dried at 120 °C for 4 hours. Subsequently, 50 grams of dry, fine red mud were mixed homogeneously with fine coal and additives with particle sizes less than 100 mesh. The mixture was agglomerated into a pellet with a 10 mm diameter and heated in a muffle furnace with atmospheric air at 1050-1250 °C for 60 minutes. Furthermore, the reduced pellets were rapidly quenched in water, dried, and ground to less than 147 µm (200-mesh). A fine reduced mixture was subjected to wet magnetic separation using a roll magnetic separator with a 500 Gauss magnetic field to separate a magnetic particle-rich in metallic iron, called concentrate, from a non-magnetic particle-rich in impurities, called tailing. The tailing was resubmitted to the magnetic separation process three times to ensure no magnetic iron phase in the tailing.

Table 2. Proximate analysis, ash composition and sulfur content of coal.

Proximate analysis (wt%)				Ash Composition (wt%)				Sulfur Content (wt%)
Fix carbon	Moisture content	Volatile matter	Ash	SiO_2	Al_2O_3	K_2O	CaO	
64.55	0.78	21.10	13.55	49.13	21.84	0.92	0.89	2.68

Analysis Procedure

X-Ray Fluorescence (XRF) analysis was used to determine the iron grade in the concentrate and tailings. It is also used to calculate the recovery of iron from Equation (9). The X-Ray Diffractometer (XRD) and Secondary Electron Microscope equipped with an Electron Discharge Spectrometer were used to analyze the phase transformation and particle size of metallic iron in a reduced pellet. The metallization analysis was performed by dissolving a concentrate in iron(III) chloride, then titrating with potassium dichromate solution (IS 15774: 2007). The concentrate's metallization degree was obtained using Equation (10). For XRF and XRD, the sample was prepared as a loose powder with a particle size less than 147 µm. For SEM-EDS, samples were mounted in resin and polished using paper grit #4000.

$$\text{Recovery Fe (\%)} = \frac{\text{Fe grade (\%)} \cdot \text{weight of concentrate}}{\text{Fe total (\%)} \cdot \text{weight of red mud}} \quad (9)$$

$$\text{Metalization degree (\%)} = \frac{\text{Fe metal in concentrate (g)}}{\text{Fe total (\%)} \cdot \text{weight of red mud}} \quad (10)$$

RESULTS AND DISCUSSION

Carbothermic Reduction Process of Red Mud without Additives

In this first section, the effect of reductant dosage in the carbothermic reduction of red mud was carried out without additives. The reduction was carried out at 1150 °C for 60 minutes. From Figure 2, the metallization degree and iron recovery increase with increasing reductant dosage from 0.2 to 1.0 times the stoichiometric amount. Increasing reductant availability can promote metallic iron formation by increasing CO gas, which could enhance atmospheric reduction (Xiao et al., 2022). However, further addition of reductant to 1.6 times the stoichiometric amount results in an insignificant increase in the degree of metallization, while recovery declines. Using coal as a reductant leaves ash, mainly containing silica and alumina. Therefore, more coal addition will increase impurities. It will inhibit the reduction of iron oxide into metallic iron. In this work, the optimum reductant dosage was 1.0 stoichiometric, which yielded metallization degree, grade, and iron recovery in the concentrate of 67.70%, 48.04%, and 55%, respectively.

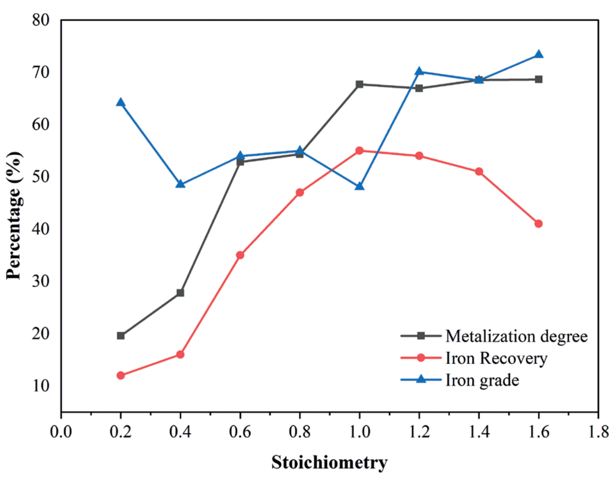

Figure 2. Effect of reductant dosage on carbothermic reduction of red mud.

The qualitative and quantitative XRD analyses of the reduced pellet are shown in Figure 3 and Table 3, respectively. From both analyses, magnetite and wustite decrease with increasing reductant dosage. They are transformed into metallic iron. However, the amount of reductant increases to 1.6 times the stoichiometric amount, and the wustite increases again. It indicates that hematite is hardly reduced to the metallic state, as evidenced by the greater ash content at higher coal dosages. Coal also contains sulfur, which could react with iron to form troilite (FeS). Table 3 shows that troilite increases with increasing reductant dosage. Troilite is also observed in Figure 3. Troilite has a low eutectic melting point of 980 °C. The low melting point of troilite promotes the formation of a liquid phase, thereby reducing the diffusion of carbon monoxide gas and enabling the reduction of iron oxide and silicate to Fe metal. Conversely, the formation of non-magnetic troilite may also slow down the metallization of iron (Nurjaman et al., 2021). Troilite mineral has non-magnetic properties. Therefore, the troilite cannot be attracted by a magnet during magnetic separation; thus, it enters the tailings. It also contributed to the low iron recovery when the reductant dosage exceeded the stoichiometric value of 1.0. Nepheline or sodium-aluminosilicate is also observed in Figure 3. Sodium comes from the alkali caustic during the Bayer process. In this high-temperature process, sodium is reacted with SiO_2 and Al_2O_3 to form nepheline. It also has a lower melting point, which could enhance iron particle agglomeration and improve iron recovery.

Microstructural analysis of reduced ore was performed to investigate the formation of iron particles after reduction, as illustrated in Figure 4. A white area indicates the presence of metallic iron particles. Other particles surrounding the metallic iron are also observed, where gray and dark areas are identified as impurities. From Figure 4a, wustite is observed as a gray area, indicating the incomplete reduction process due to the limitation of reductant dosage. Some iron oxide is also associated with sodium, aluminum and titanium. Only a small amount of metallic iron is found. The particle size of iron increases with the increase in reductant dosage. No more wustite

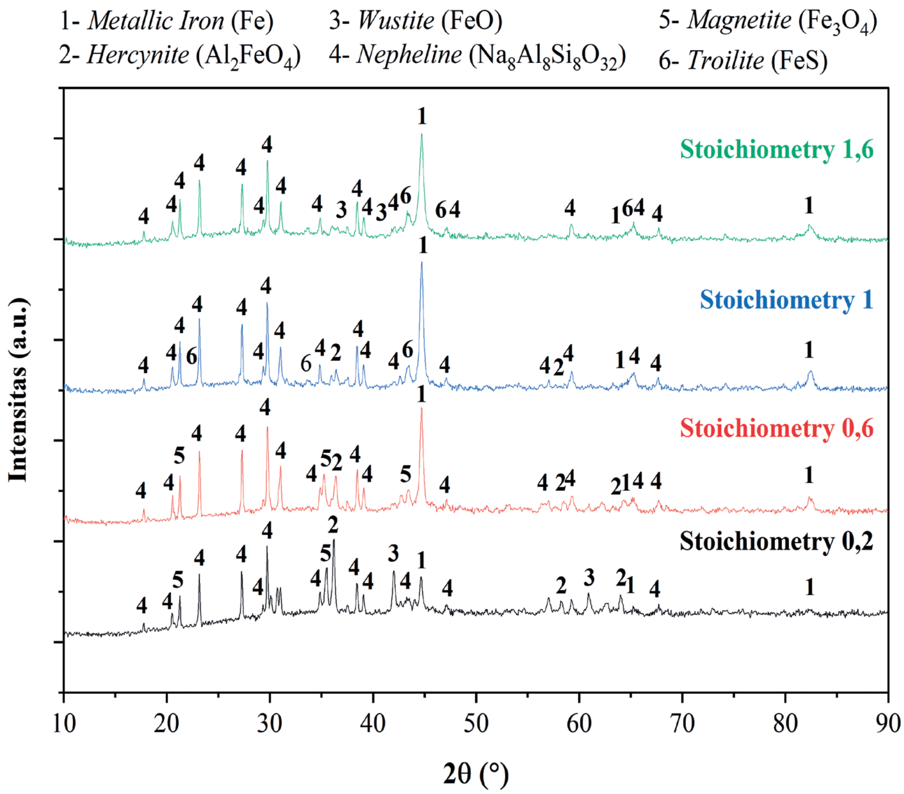

Figure 3. XRD analysis of carbothermic reduction of red mud with various dosages of reductant [1-Iron (Fe); 2-Hercynite (Al_2FeO_4); 3-Wustite (FeO), 4-Nepheline ($NaAlSiO_4$), 5-Magnetite (Fe_3O_4), 6-Troilite (FeS), 7-Fayalite (Fe_2SiO_4)].

Table 3. The Rietveld analysis of XRD from reduced ore with various reductant dosages.

Metal/Mineral	Formula	Stoichiometry of carbon in the reductant			
		0.2	0.6	1.0	1.6
Iron	Fe	4.6	14.1	19.9	21.6
Hercynite	Al_2FeO_4	16.5	12.9	5.4	-
Wustite	FeO	11.6	-	-	4.6
Nepheline	$NaAlSiO_4$	50.5	58.4	71.6	63.6
Magnetite	Fe_3O_4	16.2	14	-	-
Troilite	FeS	-	-	1.6	10.1
Fayalite	Fe_2SiO_4	0.5	0.5	1.6	-

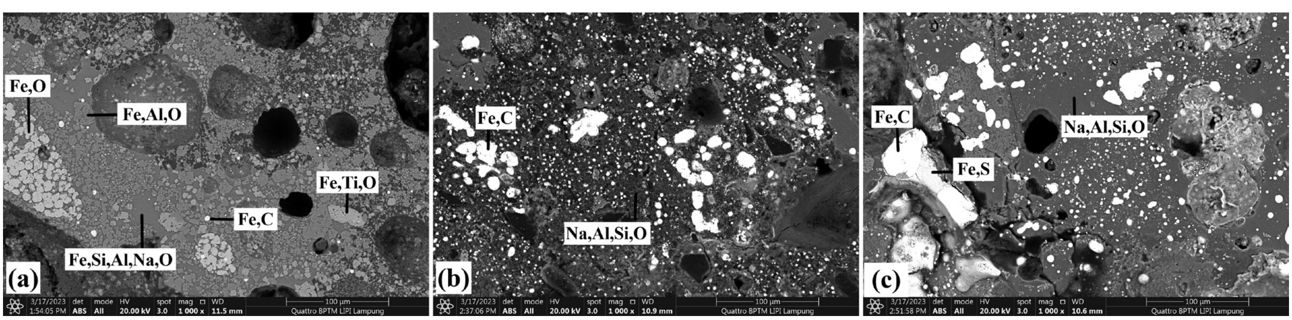

Figure 4. SEM picture of reduced pellet with various reductant dosages: (a) 0.2, (b) 1.0, (c) 1.6 stoichiometry.

is detected in Figures 4b and 4c, indicating that the iron oxide has been completely transformed into metallic iron. The impurities are mostly nepheline, a sodium, aluminum, and silicon oxide. Troilite is observed in Figure 4c. It contributes to the agglomeration of iron particles. Nevertheless, it negatively affects iron recovery.

Effect of Additives: $CaCl_2$ and CaF_2

In this section, the effect of additives on the carbothermic reduction of red mud was investigated clearly. The optimum reductant dosage of 1.0 stoichiometry was used. The reduction was carried out at 1150 °C for 60 minutes. The iron grade, recovery, and metallization degree increase with increasing CaF_2 dosage, as shown in Figure 5. The iron grade increases significantly from 0% to 2% CaF_2, and no significant change occurs until 10% CaF_2 is added. The optimal metallization degree is obtained at 8% CaF_2, corresponding to 90.83%. As shown in Figure 1 and Table 1, red mud contains high SiO_2, which tends to react with FeO to form Fe_2SiO_4, as expressed in Reaction (11). This iron silicate phase is more difficult to reduce to metallic iron by carbothermic reduction than iron oxide. Therefore, red mud without additives showed lower recovery than with CaF_2 addition. From Reaction (13), CaF_2 can be reacted with SiO_2 to prevent the formation of Fe_2SiO_4. According to Zhao et al. (2021), F- ions can more easily replace the position of O_2- because both have a similar atomic radius. F- ions can disrupt the iron matrix in red mud, reducing the lattice stability and thereby enhancing the reduction process. CaF_2 can also react with iron olivine in red mud to release iron, forming FeF_2, as expressed in Reaction (15). It has a low melting point, which enhances mass transfer, reduces resistance to migration processes, and promotes the incorporation of metallic iron (Cao et al., 2022). The optimum result for the CaF_2 additive was established at 8%, with iron grade, recovery and metallization degree of 87.698%, 86.22%, 90.83%, respectively.

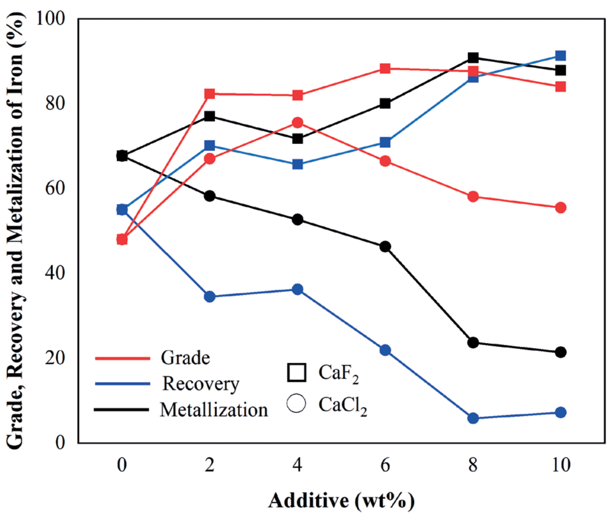

Figure 5. Effect of additives on carbothermic reduction of red mud.

$$FeO+SiO_2 \rightarrow Fe_2SiO_4 \quad (11)$$

$$Fe_2SiO_4+2C \rightarrow 2Fe+SiO_2+2CO_{(g)} \quad (12)$$

$$2CaF_2+SiO_2 \rightarrow 2CaO+SiF_4 \quad (13)$$

$$CaO+SiO_2 \rightarrow CaSiO_3 \quad (14)$$

$$Fe_2SiO_4+2CaF_2+2C \rightarrow 2SiO_3+FeF_2+2FeSi_2+2CO_{(g)} \quad (15)$$

On the contrary, with the increasing addition of the additive $CaCl_2$, iron's recovery and metallization degree continuously decrease, while the iron grade increases until 4% $CaCl_2$. During the reduction roasting process, calcium chloride reacts with the silicon dioxide and crystal water to form hydrochloric acid, as expressed in Reaction (17) (Xiao et al., 2019). It will inhibit the formation of iron silicate. However, a chlorination reaction occurs between hydrochloric acid and iron oxide to form iron (II) chloride ($FeCl_2$), as shown in Reaction (18), which has a boiling point of 1023 °C. Therefore, $FeCl_2$ gas will be generated during the reduction process at 1150 °C. From the mass balance of iron, as expressed in Table 4, the carbothermic reduction with $CaCl_2$ resulted in higher iron losses than with CaF_2, indicating that $FeCl_2$ gas was formed. Low recovery and iron metallization with the increasing $CaCl_2$ addition indicate that more $FeCl_2$ gas is generated. Optimum results are obtained by adding 2% $CaCl_2$ to red mud, with metallization degree, grade, and iron recovery of 58.28%, 67%, and 34.55%, respectively.

$$C+H_2O_{(g)} \rightarrow CO_{(g)}+H_{2(g)} \quad (16)$$

$$CaCl_2+SiO_2+H_2O_{(g)} \rightarrow CaO \cdot SiO_2+2HCl_{(g)} \quad (17)$$

$$FeO+HCl_{(g)} \rightarrow FeCl_{2(g)}+H_2O_{(g)} \quad (18)$$

$$2CaCl_2+Al_2O_3 \cdot 2SiO_2 2H_2O \rightarrow (CaO)_2 2SiO_2 2H_2O+4HCl_{(g)} \quad (19)$$

$$FeCl_2+H_{2(g)} \rightarrow Fe+HCl_{(g)} \quad (20)$$

$$FeTiO_3+HCl \rightarrow FeCl_2+TiOCl_2+H_2O_{(g)} \quad (21)$$

$$8NaAlSiO_4+CaCl_2+CO_2 \rightarrow Na_8Al_6S_6O_{24}Cl_2+CaAl_2S_2O_8 \quad (22)$$

Table 4. Mass balance of total iron during the magnetic separation process.

Additive (wt%)	Mass of iron before magnetic separation (g)	Mass of iron in concentrate + tailing (g)	Percentage of iron losses (%)
CaF_2			
2	9.58	9.54	0.4
4	8.84	8.79	0.6
6	8.88	8.67	2.4
8	7.88	7.85	0.4
10	7.51	7.45	0.8
$CaCl_2$			
2	10.70	8.82	17.6
4	11.55	10.09	12.6
6	14.10	11.49	18.5
8	10.62	9.10	14.3
10	8.72	8.17	6.3

The qualitative and quantitative XRD analysis results for reduced pellets with various additives are presented in Figure 6 and Table 5, respectively. Metallic iron is observed when using CaF_2 or $CaCl_2$ additives. It increases with increasing CaF_2, while it decreases with increasing $CaCl_2$. It is explained by Reaction (18), which resulted in a low recovery and a low metallic degree of iron using $CaCl_2$. Nepheline ($NaAlSiO_4$), which is generated from the decomposition of natrolite, as expressed in Reaction (7), was reacted with $CaCl_2$ to form sodalite ($Na_8Al_6Si_6O_{24}Cl_2$) and anorthite ($CaAl_2Si_2O_8$) as appeared in the XRD pattern (Figure 6). According to Xiao et al. (2020), the reaction of magnesium, sodium, aluminum, and potassium oxides with hydrochloric acid gas to form magnesium chloride, potassium chloride, and sodium chloride can reduce the efficiency of the subsequent reduction process. It is indicated by the presence of magnetite containing titanium in 2% CaF_2 addition. Therefore, the recovery and metallization of iron are low, although the iron in impurities has been replaced by chlorine. Nevertheless, sodalite has a low melting point, i.e., 1079 °C (Antao and Hasan, 2002). Thus, it could enhance the agglomeration of metallic

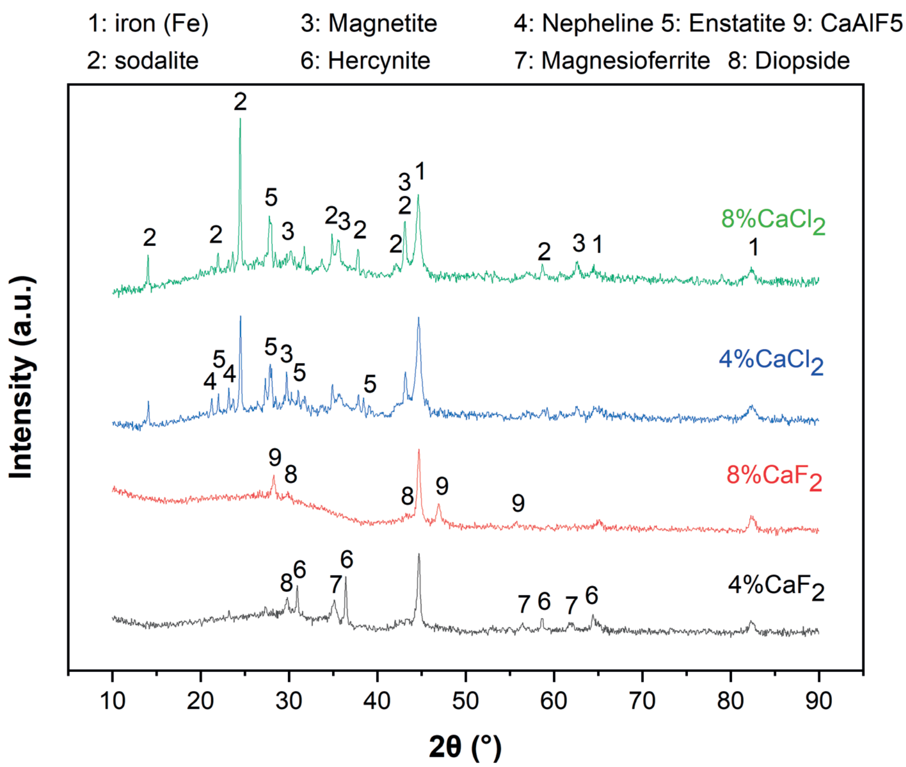

Figure 6. XRD analysis of various additives in carbothermic reduction of red mud at a reduction temperature of 1250 °C. (1-iron (Fe), 2-sodalite [$Na_8(Al_6Si_6O_{24})C1_2$], 3-magnetite (Fe_2TiO_4), 4-nepheline ($NaAlSiO_4$), 5-anorthite ($CaAl_2Si_2O_8$), 6-hercynite ($FeAl_2O_4$), 7-iron fluoride (FeF_2), 8-Diopside ($CaSiO_3$), 9-calcium fluoride (CaF_2).

Table 5. The Rietveld analysis of XRD from reduced ore with various additives.

Metal and Mineral	Formula	Additive			
		4% CaF_2	8% CaF_2	4% $CaCl_2$	8% $CaCl_2$
Iron	Fe	9.7	15.9	15.5	12.9
Sodalite	$Na_8(Al_6Si_6O_{24})Cl_2$	-	-	18.3	25.0
Magnetite (Titanium)	Fe_2TiO_4	-	-	-	12.4
Nepheline	$NaAlSiO_4$	-	-	25.6	-
Anorthite	$CaAl_2Si_2O_8$	-	-	40.5	49.8
Hercynite	Al_2FeO_4	17.8	-	-	-
Iron Fluoride	FeF_2	1.3	31.2		
Diopside	$CaSiO_3$	71.2	33.4	-	-
Calcium fluoride	CaF_2	-	19.6	-	-

iron particles. It differs from anorthite, which has a high melting point, i.e., 1550 °C (Wu et al., 2022).

By using CaF_2, diopside ($CaSiO_3$) appears due to the reaction of calcium oxide with SiO_2 from Reaction (14), which inhibits the formation of fayalite. Hercynite is identified with the addition of 4% CaF_2. It can be formed from the Reaction of iron oxide and aluminum oxide, as expressed in Reaction (6). Nevertheless, hercynite is not detected at 8% CaF_2. However, aluminum can be present as a solid solution in diopside by substituting for silicon, which could explain the absence of hercynite in 8% CaF_2. Iron fluoride (FeF_2) diffraction is shown in Figure 6. As mentioned above, it will provide an advantage in high iron recovery by promoting the agglomeration of iron particles. Therefore, the recovery of iron increases with the increase in CaF_2. The presence of CaF_2 diffraction at 8% CaF_2 addition indicates excessive CaF_2 has been added.

SEM-EDS analysis for the reduced pellet with additives is given in Figure 7. The particle of metallic iron resulting from carbothermic reduction of red mud with CaF_2 addition is larger than that of $CaCl_2$. Its size increases with the increasing additive dosage. Agglomerations of metallic iron occurred due to the low melting point, with the liquidus phase generated during the reduction process at elevated temperature. By using a CaF_2 additive, FeF_2 forms a low-melting-point phase at 970 °C, which contributes to the agglomeration of metallic iron particles (Cao et al., 2022). However, due to the small amount of phase present, FeF_2 is not identified in the XRD analysis in Figure 6, but it is sufficient to promote the increase in particle size of iron. The presence of FeF_2 could be correlated with the presence of iron and fluorite in impurities (dark color) in Figure 7(c-d). However, the liquidus phase can also be analyzed from the lower pore volume observed in CaF_2 addition compared with $CaCl_2$. From Figure 7a, adding 2% $CaCl_2$ could not release titanium from iron-titanium oxide ($FeTiO_3$), resulting in low iron recovery. This phenomenon is similar to using 0.2 stoichiometric without additives (Figure 4a). Extraction of iron from titanium using chloric acid (HCl) has been well reported, as shown in Reaction (21) (Sun et al., 2024; Haverkamp et al., 2016). In this experiment, HCl will be produced via Reaction (17). Therefore, it needs sufficient $CaCl_2$ to separate iron from iron-titanium oxide. As illustrated in Figure 7b, the titanium is present as an impurity oxide in a dark matrix, together with sodium, silicate, and aluminum, indicating that the titanium could be released from the iron oxide structure at higher $CaCl_2$ dosages during the reduction of red mud.

Effect of Temperature Reduction

This section studied the effect of temperature on carbothermic reduction of red mud with the addition of $CaCl_2$ and CaF_2. The optimum additives from the previous section, i.e., 2% $CaCl_2$ and 8% CaF_2, were used. The optimum reductant stoichiometry of 1.0 was used, and the reduction was carried out at 1050-1250 °C for 60 minutes.

Figure 8 shows that temperature positively affects the iron grade, recovery, and metallization degree in the carbothermic reduction of red mud with $CaCl_2$ and CaF_2 additions. Increasing temperature increases the rate of reduction of iron oxide to metallic iron. It also enhances the migration and diffusion of metallic iron, which promotes the agglomeration and growth of metallic iron particles. The optimum grade, recovery, and metallization degree of iron obtained for both samples were 1250 °C. For 2% $CaCl_2$, the values are 83.41%, 78%, and 81.58%, respectively. Higher values are obtained for 8% CaF_2: 83.64%, 98%, and 93.5%.

From Figure 9 and Table 6, the carbothermic reduction of red mud at 1250 °C with $CaCl_2$ produced sodalite and iron, which dominate in the reduced pellet. A corundum

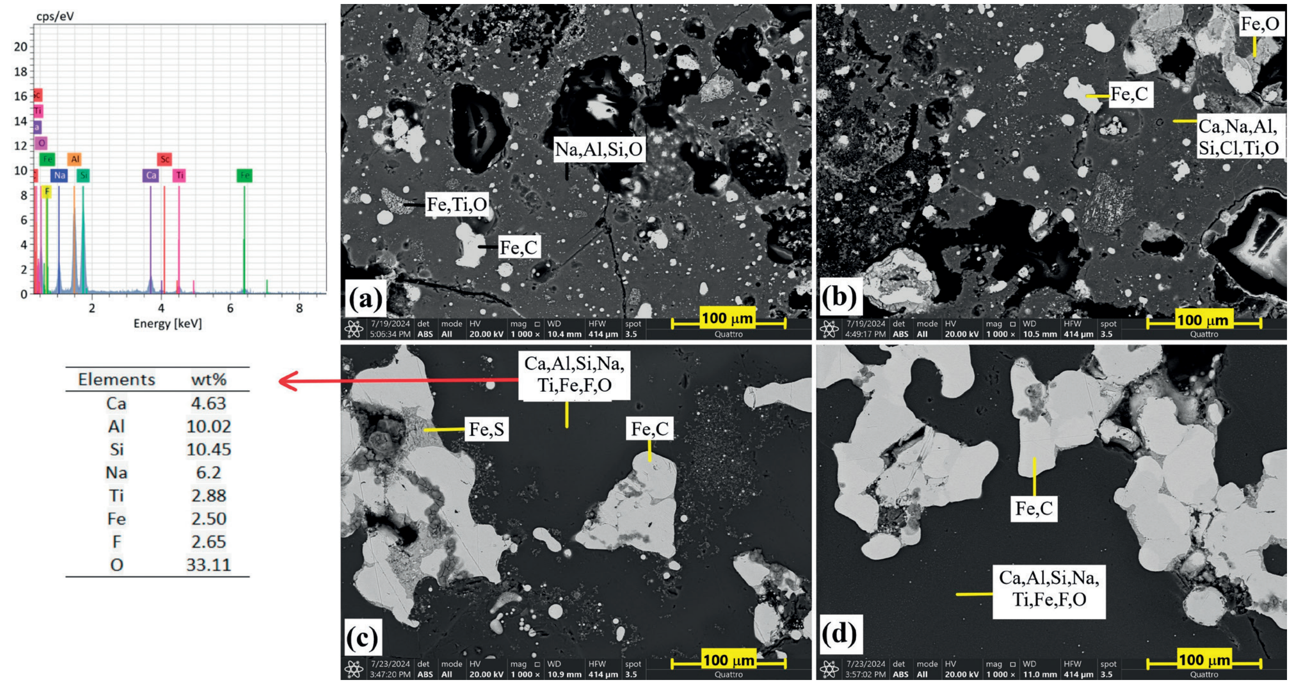

Elements	wt%
Ca	4.63
Al	10.02
Si	10.45
Na	6.2
Ti	2.88
Fe	2.50
F	2.65
O	33.11

Figure 7. SEM-EDS picture of reduced pellet with various additives at reduction temperature of 1150 °C: (a) 4% $CaCl_2$, (b) 8% $CaCl_2$, (c) 4% CaF_2, (d) 8% CaF_2.

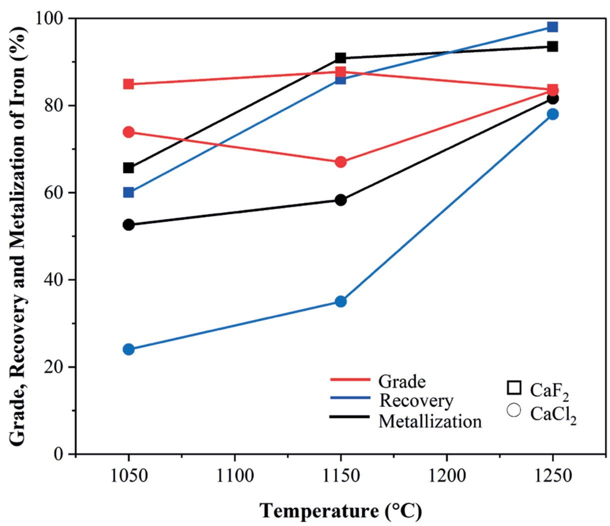

Figure 8. Effect of reduction temperature on carbothermic reduction of red mud.

or aluminum oxide (Al_2O_3) has been observed as a new phase. Chlorination of iron and impurities associated with aluminum oxide appears to be faster at higher temperatures. Thus, it leaves aluminum oxide, which potentially could be processed to obtain pure aluminum oxide from red mud. By using CaF_2 at 1250 °C, no new phase is observed. However, diopside dominates. FeF_2 is less than when the carbothermic reduction is carried out at 1150 °C (Table 5). It is indicated that iron oxide tends to transform into metallic iron at higher reduction temperatures.

From the SEM pictures, the metallic iron particle (bright color) in Figure 10 is larger than that in Figure 7, for both $CaCl_2$ and CaF_2 additives. It is clear that increasing the temperature will promote the growth of metallic iron particles because the reduction rate of iron oxide increases. It could also be observed that the particle size of metallic iron obtained from using 8% CaF_2 is larger than 2% $CaCl_2$, which indicates that the presence of the liquidus phase will enhance the agglomeration of metallic iron. The larger size of the metallic iron particles increases their degree of liberation from impurities (as shown by the dark color). Thus, enhancing the recovery of the obtained iron.

CONCLUSION

Metallic iron has been successfully extracted from red mud via carbothermic reduction, followed by magnetic separation. Increasing the reductant dosage can improve the metallization degree and recovery of iron. The optimal result was obtained with a 1.0 stoichiometric ratio. Nevertheless, excessive reductant dosage has negatively affected the pellet mixture, leading to higher ash and sulfur content as coal addition increases, resulting in higher

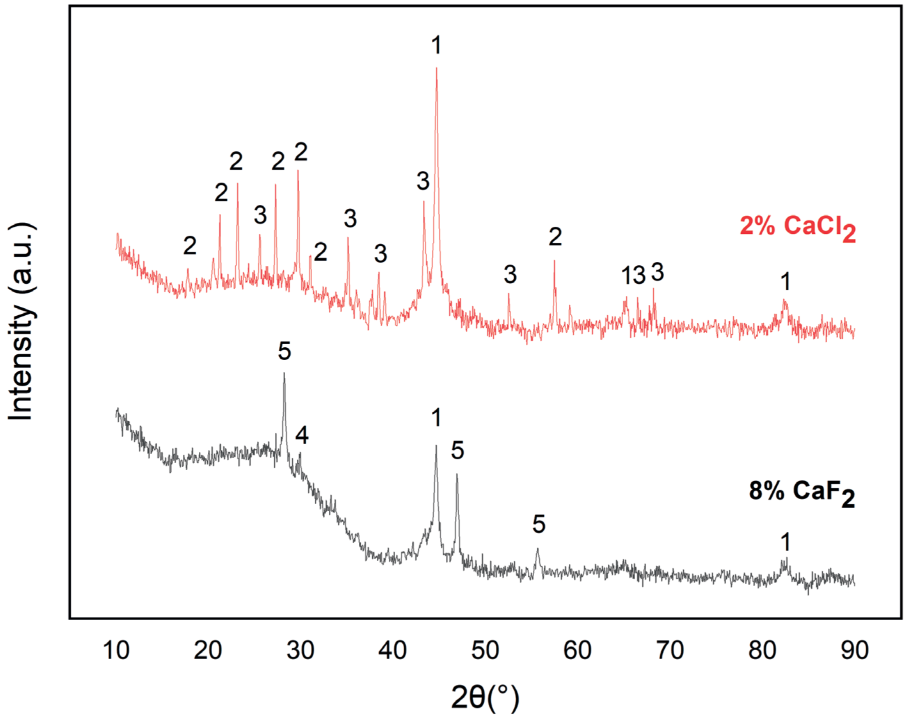

Figure 9. XRD analysis of optimum additives at a reduction temperature of 1250 °C. (1-iron (Fe), 2-nepheline ($NaAlSiO_4$), 3-corrundum (Al_2O_3), 4-diopside ($CaSiO_3$), 5-calcium fluoride (CaF_2), 6-iron fluoride (FeF_2).

Table 6. The Rietveld analysis of XRD from reduced ore at a reduction temperature of 1250 °C.

Metal and Mineral	Formula	Additive	
		2% $CaCl_2$	8% CaF_2
Iron	Fe	17,4	16.6
Nepheline	$NaAlSiO_4$	43.4	-
Corrundum	Al_2O_3	39.2	-
Diopside	$CaSiO_3$	-	54.4
Calcium fluoride	CaF_2	-	27.5
Iron Fluoride	FeF_2	-	1.5

impurities and a troilite phase that could suppress the iron's metallization degree and recovery. Using additive CaF_2, used as an additive in red mud's carbothermic reduction, increased the metallization degree and recovery of metallic iron. Their enhancement is due to the inhibition of iron silicate and the formation of the liquidus phase, with $CaSiO_3$ and FeF_2, respectively. The presence of liquidus phases promotes the agglomeration of iron particles. Thus, it positively affected iron recovery. However, adding $CaCl_2$ to this carbothermic reduction process yields the opposite result to that with CaF_2. The chlorination effect is not very effective at enhancing recovery and metallization during red mud reduction because $FeCl_2$ gas forms at high temperatures, leading to iron vaporization. In this work, the optimal results for iron grade, recovery, and metallization of iron from carbothermic reduction of red mud are 83.64%, 98%, and 93.5%, respectively. It was obtained by adding 8% CaF_2 and 1,0 stoichiometric amount of reductant to the red mud, which was heated at 1250 °C for 60 minutes.

ACKNOWLEDGEMENTS

The authors would like to thank the Universitas Indonesia for funding this research through Hibah Profesor 2024/2025, contract number NKB-3451/UN2.F4.D/PPM.00.00/2024, and the National Research and Innovation Agency of Indonesia for research facilities and technical support.

Conflict of interest

On behalf of all authors, the corresponding author confirms that there is no conflict of interest.

REFERENCES

Agrawal S., Rayapudi V., Dhawan N., 2018. Microwave reduction of red mud for recovery of iron values. Journal of Sustainable Metallurgy 4, 427-436.

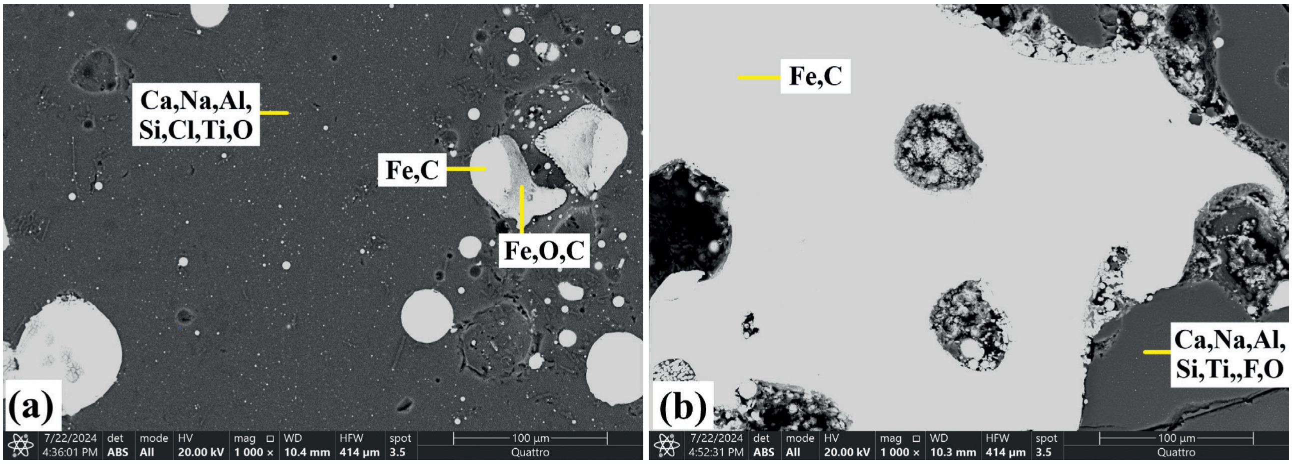

Figure 10. SEM-EDS analysis for reduced pellet at reduction temperature of 1250 °C: (a) 2% $CaCl_2$ and (b) 8% CaF_2.

Antao S.M., Hassan I., 2002. Thermal analysis of sodalite, tugtupite, danalite and helvite. The Canadian Mineralogist 40, 163-172.

Arroyo F., Luna-Galiano Y., Leiva C., Vilches L.F., Fernadez-Pereira C., 2020. Environmental risks and mechanical evaluation of recycling red mud in bricks. Environmental Research 186, 109537, 1-8.

Balomenos E., Kastritis D., Panias D., Paspaliaris I., Boufounos D., 2014. The enexal bauxite residue treatment process industrial scale pilot plant results. Light Met. 143-147.

Bhoi B., Rajpur P., Mishra C.R., 2017. Production of grenn direct reduced iron (DRI) from red mud of Indian origin: A novel concept. Proceedings of 35th International ICSOBA Conference, Hamburg, Germany, 565-574.

Borra C.R., Blanpain B., Pontikes Y., Binnemans K., Gerven T.V., 2016. Smelting of bauxite residue (red mud) in view of iron and selective rare earths recovery. Journal of Sustainability Metallurgy 2, 28-37.

Yi X., Lu Y., He G., 2024. Aluminum demand and low carbon development scenarios for major countries by 2050. Journal of Cleaner Production 475, 143647, 1-11.

Cao Z., Ma B., Zhou J., Chen Y., Wang C., 2022. The study for reduction roasting of laterite residue in the presence of CaF2. Process Safety and Environmental Protection 168,1-9.

Chun T.j., Zhu D.Q., Pan J., He Z., 2014. Preparation of metallic iron powder from red mud by sodium salt roasting and magnetic separation. Canadian Metallurgical Quarterly 53, 183-189.

Ding W., Xiao J., Peng Y., Shen S., Chen T., Zou K., Wang Z., 2020. A novel process for extraction of iron from a refractory red mud. Physicochemical Problems of Mineral Processing 56 (6), 125-136.

Dmitriev A., 2018. The comprehensive utilization of red mud utilization in blast furnace. Chapter Book: Recovery and utilization of metallurgical solid waste, 1-13.

Eray S., Kekinkilic E., Topkaya Y.A., Geveci A., 2021. Reduction behavior of iron in the red mud. Journal of Mining and Metallurgy, Section B: Metallurgy,57, 431-437.

Grudinsky P., Zinoveev D., Yurtaeva A., Kondratiev A., Dyubanov,V., Petelin A., 2021. Iron recovery from red mud using carbothermic roasting with addition of alkaline salts. Journal of Sustainable Metallurgy 7, 858–873.

Haverkamp R.G., Kruger D., Rajashekar R., 2016. The digestion of New Zealand ilmenite by hydrochloric acid. Hydrometallurgy 163, 198-203.

Joseph C.G., Taufiq-Yap Y.H., Krishnan V., Puma G.L., 2020. Application of modified red mud in environmentally-benign application: A review. Environmental Engineering Research 25, 795-806.

Liu X., Han Y., He F., Gao P., Yuan S., 2021. Characteristic, hazard and iron recovery technology of red mud-A critical review. Journal of Hazardous Materials 420, 126542, 1-13.

Li G., Liu M., Rao M., Jiang T., Zhuang J., Zhang Y., 2014. Stepwise extraction of valuable components from red mud based on reductive roastingwith sodium salts. Journal of Hazardous Materials 280, 774-780.

Mombelli D., Mapelli C., Barella S., Gruttadauria A., Spada E., 2019. Jarosite wastes reduction through blast furnace sludges for cast iron production. Journal of Environmental Chemical Engineering, 7, p. 102966.

Ning G., Zhang B., Liu C., Li S., Ye Y., Jiang M., 2018. Large-scale consumption and zero-waste recycling method of red mud in steel making process. Minerals 102, 1-16.

Nurjaman F., Astuti W., Bahfie F., Suharno B., 2021. Study of selective reduction in lateritic nickel ore: Saprolite versus limonite," Mater Today Proc 44, 1488-1494.

Paramguru R.K., Rath P.C., Mishra V.N., 2004. Trends in red mud utilization-A review. Mineral Processing and Extractive Metallurgy Review: An International Journal 26, 1-29.

Paramguru R.K., Rath P.C., Mishra V.N., 2004. Trends in red mud utilization-A review. Mineral Processing and Extractive Metallurgy Review: An International Journal 26, 1-29.

Sadangi J.K., Das S.P., Tripathy A., Biswal S.K., 2018. Investigation into recovery of iron values from red mud dumps. Separation Science and Technology 53, 2186-2191.

Samouhos M., Taxiarchou M., Pilatos G., Tsakiridis P.E., Devlin, E., Pissas M., 2017. Controlled reduction of red mud by H2 followed by magnetic separation. Miner. Eng. 105, 36-43.

Sun T.Y., Wykes J.L., Wolmarans K., Kappen P., Haverkamp R.G., 2024. The dependence of ilmenite's dissolution rate in hydrochloric acid on the Fe(III)/Fe(II) ratio, with Fe K-Edge XANES pre-edge peak analysis. Minerals 15, 20, 1-10.

Swain B., Akcil A., Lee J., 2020. Red mud valorization an industrial waste circular economy challenge; review over processes and their chemistry. Critical Reviews in Environmental Science and Technology, 1-51.

Wang M. and Liu X., 2021. Applications of red mud as an environmental remediation material: A review. Journal of Hazardous Materials 408, 124420, 1-13.

Valeev D., Zinoveev D., Kondratiev A., Lubyanoi D., Pamkratov D., 2020. Reductive smelting of neutralized red mud for iron recovery and produced pig iron for Heat-Resistant Castings. Metals, 10 (32), 1-20.

Wang S., Jin H., Deng Y., Xiao Y., 2021. Comprehensive utilization status of red mud in China: A critical review. Journal of Cleaner Production 289, 125136, 1-13.

Wang M. and Liu X., 2021. Applications of red mud as an environmental remediation material: A review. Journal of Hazardous Materials 408, 124420, 1-13.

Wu J., Yu J., Xu X., Liu Y., Zhang Z., Wei P., 2022. Preparation and thermal shock resistance of anorthite solar thermal energy storage ceramics from magnesium slag. Ceramics International 48, 33604-33614.

Xiao J., Zhong N., Gao D., Zou K., Wang Z., Huang W., Xiong W., 2022. An efficient process to recover iron from bayer red mud. JOM, 74, 3172-3180.

Xiao J., Ding W., Peng Y., Wu Q., Chen Z., Wang Z., Wang J., Peng T., 2019. Upgrading iron and removing phosphorus of high phosphorus oolitic iron ore by segregation roasting with calcium chloride and calcium hypochlorite. Journal of Mining and Metallurgy, Section B: Metallurgy, 55, 305-314.

Xiao J., Ding W., Peng Y., Chen T., Zou K., Wang Z., 2020. Extraction of nickel from garnierite laterite ore using roasting and magnetic separation with calcium chloride and iron concentrate. Minerals 10, 352.

Yadav S.V., Prasad M., Khan J., Amrithpale S,S., Singh M., Raju C.B., 2010. Sequestration of carbon dioxide (CO_2) using red mud. Journal of Hazardous Materials 176, 1044-1050.

Yi X., Lu Y., He G., 2024. Aluminum demand and low carbon development scenarios for major countries by 2050. Journal of Cleaner Production 475, 143647, 1-11.

Zhao Y., Sun T., Wang Z., 2021. Extraction of iron from refractory titanomagnetite by reduction roasting and magnetic separation. ISIJ International, 61, 93-99.

Zhou J., Dai M., Guan Q., Zeng H., Sun W., Wang Li., 2024. Optimizing the dealkalization process of red mud: Controlling calcium compounds to improve solid-liquid separation performance. Minerals 15, 150, 1-15.

Zhu D., Chun T., Pan J., He Z., 2012. Recovery of iron from high-iron red mud by reduction roasting with adding sodium salt. Journal of iron and steel research, International 19(8), 1-6.